

# Tunable photonic thermal rectification through a superconducting artificial atom

Jorden Senior,<sup>\*</sup> Azat Gubaydullin, Bayan Karimi, Joonas T. Peltonen, and Jukka P. Pekola

*QTF Centre of Excellence, Department of Applied Physics,*

*Aalto University School of Science,*

*P.O. Box 13500, 00076 Aalto, Finland*

---

<sup>\*</sup> jorden.senior@aalto.fi

Controlling heat transport in superconducting circuits and devices is topic of increasing relevance in engineering microwave environments for circuit quantum electrodynamics (cQED), and circuit quantum thermodynamics experiments (cQTD), and directly for engineering thermal logic and caloritronic devices. The anharmonic two-level system artificial atom tunably coupled to two thermal baths is a optimal tool for studying tunable heat transport and rectification, thermally analogous to the electronic transistor and diode, themselves revolutionary devices in the field of electronics, and can be effectively realised using elements of superconducting circuits. Utilising a superconducting transmon qubit coupled wirelessly to two superconducting coplanar waveguide (CPW) resonators, each shunted with a copper micro-strip resistor used for thermal population and bolometry was first presented as a platform for this fast-growing area of physics in [1], demonstrating flux-tunable photonic heat transport through an artificial atom coupled to two symmetric resonator-thermal baths, and highlighting the roles of the strong qubit-resonator coupling and dissipation on the locality of heat transport through the device, with a tuning ratio as high as 90%. Here, in order to study the directionality of photonic heat transport through the system, we couple the transmon qubit to two asymmetric resonators, and implement a flux-tunable wireless quantum thermal rectifier.

A rectifier is a device in which the transport through it is directionally impeded, optimally to allow transport only in one direction. In the charge transport regime, the ubiquitous charge rectifier, or diode, is one of the most fundamental tools in electronic circuits, and can be realised relatively simplistically, for example a device exploiting the depletion zone between electrons and holes in a semiconductor p-type/n-type junction. A rectifier acting in the thermal transport regime, however, is currently a topic of great interest, with many theoretical proposals of devices acting on the various carriers of heat; photons[3], phonons, and electrons, but in contrast relatively few experimental realisations[2].

The implementation of devices for manipulating charge currents is enabled by the discrete and polarised nature of the charge carrier, and their interaction with electromagnetic field. Heat currents, do not have this quality, and manipulating their flow usually rely on precise control of the energy population distributions of the various metals involved

in the device, to provide a superconducting/semiconducting gap in one direction, and/or asymmetric couplings of the heat baths to quasiparticle heat carriers, for example by using metals with differing electron-phonon couplings.

The two-level system of a transmon qubit strongly coupled to two asymmetric resonators is a well-placed tool for studying asymmetric photonic transport, with each element having engineered resonances and couplings to each other that can be designed to rectify. Moreover, by utilising a superconducting quantum interferometer (SQUID) as the non-linear element of the transmon, the qubit-resonator couplings  $g_1$  and  $g_2$ , to the left and right resonators respectively, can be tuned with the first excitation frequency  $\omega_{01}$  given by Equation 1, with the charging energy  $E_C$ , and the tunable Josephson energy  $E_J(\Phi) = E_{J0} |\cos(\pi\Phi/\Phi_0)| \sqrt{1 + d^2 \tan^2 \pi\Phi/\Phi_0}$ . Here,  $\Phi_0 = h/2e$  is the magnetic flux quantum, and  $d$  quantifies the asymmetry in the critical current of the SQUID Josephson junctions.

$$\omega_{01}(\Phi) = \frac{\sqrt{8E_C E_J(\Phi)} - E_C}{\hbar} \quad (1)$$

In the limit where the temperature differential between these thermally-populated resonators is large, and quantified by  $k_B T = 1/\beta$ , the rectification ratio  $\mathcal{R}$  of power  $P_i$  to resonator  $i$  in the forwards (+) and backwards (−) direction, is defined by Equation 2 [5].

$$\mathcal{R} = \frac{|P_i^+|}{|P_i^-|} = \frac{g_2 \coth(\frac{\beta\hbar\omega_0}{2}) + g_1}{g_1 \coth(\frac{\beta\hbar\omega_0}{2}) + g_2} \quad (2)$$

We introduce the asymmetric coupling factor  $\gamma = 1 - g_1/g_2$ , where when  $|\gamma| \ll 1$ , the rectification ratio can be simplified to Equation 3.

$$\mathcal{R} = 1 + e^{-\beta\hbar\omega_0} \gamma \quad (3)$$

Figure 1(a) presents a diagram of the realised device, consisting of a transmon qubit coupled to two resonators, designed at 3 GHz and 7 GHz respectively. Each resonator is shunted at the current maximum with a copper thin-film resistor, shown in Figure 1(b) as a colourised scanning electron micrograph, providing the thermal bath, which is heated and measured by superconducting aluminium probes. The SQUID of the transmon qubit is similarly shown in Figure 1(c).

Superconducting probes (S), separated by a thin insulator (I), are used for both thermal readout and thermal control of the copper baths (N), in a SINIS configuration. By applying a current bias between the superconducting probes close to the superconducting energy gap, hot electrons from the copper can tunnel into the superconducting probes, and a voltage signal can be measured, with a well defined dependence on the temperature of the electrons in the copper in the range 100 mK - 500 mK, of interest to this experiment. By assuming that the heat is well localised due to the near-perfect Andreev mirrors at the aluminium-copper interface, and that the main relaxation channel for the heat is via the electron-phonon coupling, the power can be estimated by  $P_{\text{el-ph}} = \Sigma V (T_{\text{el}}^5 - T_{\text{ph}}^5)$ , where  $\Sigma$  is the material dependent electron-phonon coupling constant, ( $V$ ) is volume of the copper bath, and the two temperatures correspond to the electron temperature and phonon temperature respectively. As the experiment is performed in steady-state conditions, we assume that the phonon temperature is in equilibrium with the cryostat base temperature, measured by a ruthenium oxide thermometer. Additionally, by voltage biasing the SINIS structure sufficiently above the superconducting energy gap, Joule heating of the copper can be applied, and for small voltage biasing below the gap, evaporative cooling can occur. By utilising four superconducting probes, we can both engineer the temperature of the copper bath, and measure this induced temperature in parallel.

These copper baths cause a substantial decrease in the loaded quality factor of the resonator, from an intrinsic value measured in the  $1e4$  range, to a loaded value of order  $1e1$ , which can be measured by the method presented in [6]. This quality factor is limited by the dissipation due to the resistance of the copper bath, and while lower resistance would result in higher quality resonators, with larger asymmetry in the qubit-resonator coupling, and thus stronger rectification, this would necessitate a larger volume of copper, which in turn would decrease the sensitivity of the device.

Temperature differentials between the copper baths can be applied by local Joule heating of each bath independently, thermally populating their corresponding resonator. We define the forward direction to be going from the low frequency (3 GHz) to high frequency (7 GHz) resonators, and declare the heated bath to be the source, and the heat flowing to the target bath. Temperature differentials can be applied in both the forward and reversed directions, resulting in a forward and negative heat flow accordingly, shown as a measured power on the opposite bath in Figure 2 for three source heating points, of increasing amplitude, with the

horizontal axis depicting the magnetic field applied to adiabatically tune the transmon qubit transition frequency using a global magnetic field originating from a solenoid encompassing the sample stage.

**We need to think about where the qubit zero-flux point really is here, and which peaks correspond to high coupling with which resonators.** The structure of the flux-dependent transport can be understood by estimating the tuned qubit transition frequency, with maximum power transport occurring when the qubit is tuned to the **source??** frequency. When the qubit is tuned to be in strong coupling with the 3 GHz?? resonator, however, we see a strong divergence in the signal between the forwards and backwards direction, which is then recovered when the qubit is periodically tuned. This divergence, plotted as the rectification ratio, is presented in Figure 3 for the low source heating (blue) and high source heating (purple) cases.

Here, we observe tunable photonic rectification from 0% to 12% at low thermal gradients, with an additional non-tunable rectification at higher thermal gradients, yielding  $\gamma \approx 6\%$ , or  $g_1/g_2 \approx 94\%$ .

In conclusion, we have developed a wireless thermal rectifier, the thermal counterpart to the electronic diode, utilising the anharmonic coupling of a superconducting artificial atom to two asymmetric resonators thermally populated by mesoscopic resistive baths, and have demonstrated flux-tunable rectification up-to 15%. This device is integratable with existing superconducting circuit architectures, in particular with superconducting qubits and Josephson logic, as a means of exploring the frontiers of quantum thermodynamics, and coherent caloritronics, in addition to applications in directionally manipulating heat flow in superconducting devices, for example in the fast initialisation of a qubit.

## I. ACKNOWLEDGEMENTS (USING QHV FOR NOW)

This work was funded through Academy of Finland grants 297240, 312057 and 303677 and from the European Union’s Horizon 2020 research and innovation programme under the European Research Council (ERC) programme and Marie Skłodowska-Curie actions (grant agreements 742559 and 766025). This work was supported by Quantum Technology Finland (QTF) at Aalto University. We acknowledge the facilities and technical support of Otaniemi research infrastructure for Micro and Nanotechnologies (OtaNano), and VTT

technical research centre for sputtered Nb films.

## II. AUTHOR CONTRIBUTIONS

J.S. and A.G. designed, fabricated, and measured the samples. Data analysis was performed by J.S. based on theoretical input by J.P. and B.K. J.T.P. provided technical support in both fabrication, low-temperature setups and measurements. All authors have been involved in the discussion of scientific results and implications of this work. The manuscript was written by J.S. with contributions from J.P., B.K., and A.G.

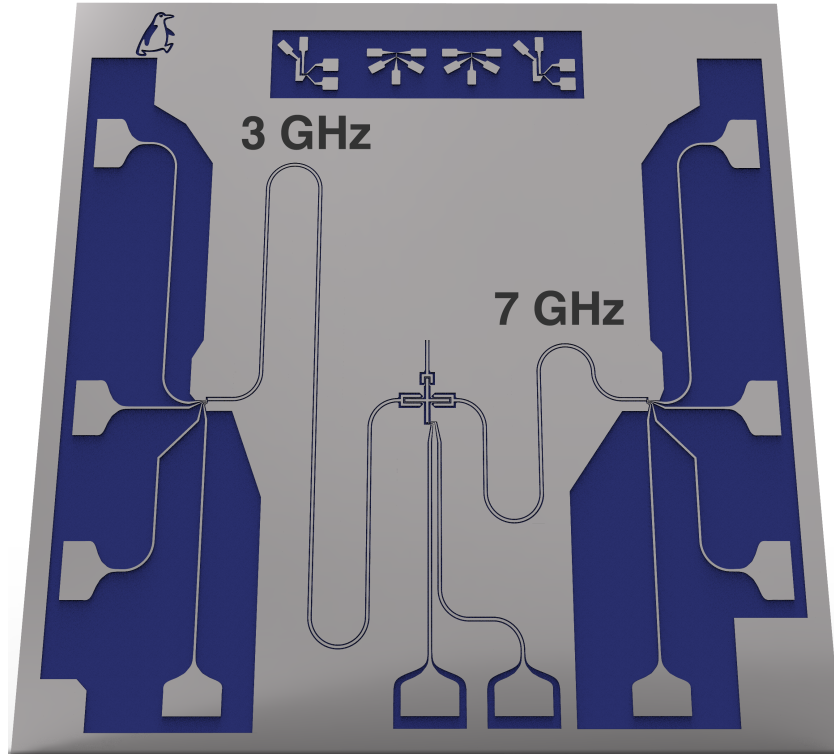
## III. COMPETING FINANCIAL INTERESTS

The authors declare no competing financial interests.

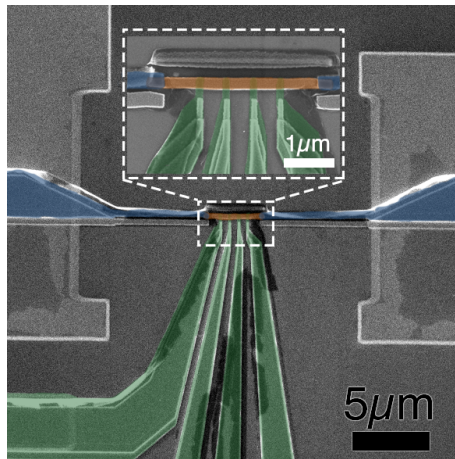
## IV. DATA AVAILABILITY

The data that support the plots within this article are available from the corresponding author upon reasonable request.

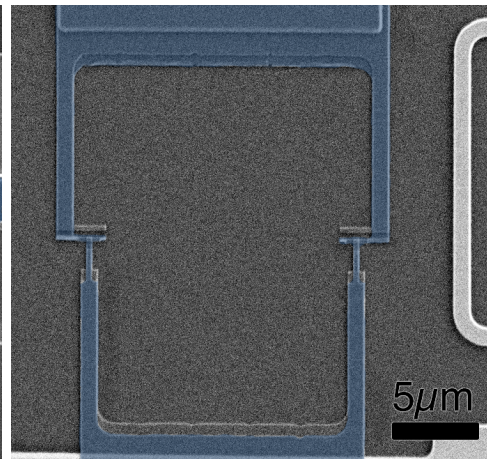
- 
- [1] Ronzani, A. *et al.* Tunable photonic heat transport in a quantum heat valve, *Nature Physics* **14**, 991-995 (2018).
  - [2] Chang, C.W. *et al.* Solid-state Thermal Rectifier, *Science* **314**, 1121 (2006).
  - [3] Ordonez-Miranda, J. *et al.* Photonic thermal diode based on superconductors, *J. Appl. Phs.* **122**, 093105 (2017).
  - [4] Fornieri, A., Martínez-Pérez, M.J., & Giazotto, F. Electronic heat current rectification in hybrid superconducting devices, *AIP Advances* **5**, 053301 (2015).
  - [5] Motz, T. *et al.* Rectification of heat currents across nonlinear quantum chains: a versatile approach beyond weak thermal contact, *New Journal of Physics* **20**, (2018).
  - [6] Chang, Y.-C. *et al.* Resistively Shunted Superconducting Resonator, in preperation , (2019).
  - [7] Sagal, D., Nitzan, A. Spin-Boson Thermal Rectifier, *Phys. Rev. Lett.* **94**, 034301 (2005).



(a)



(b)



(c)

Figure 1. A set of three figures: chip, NIS, and SQUID

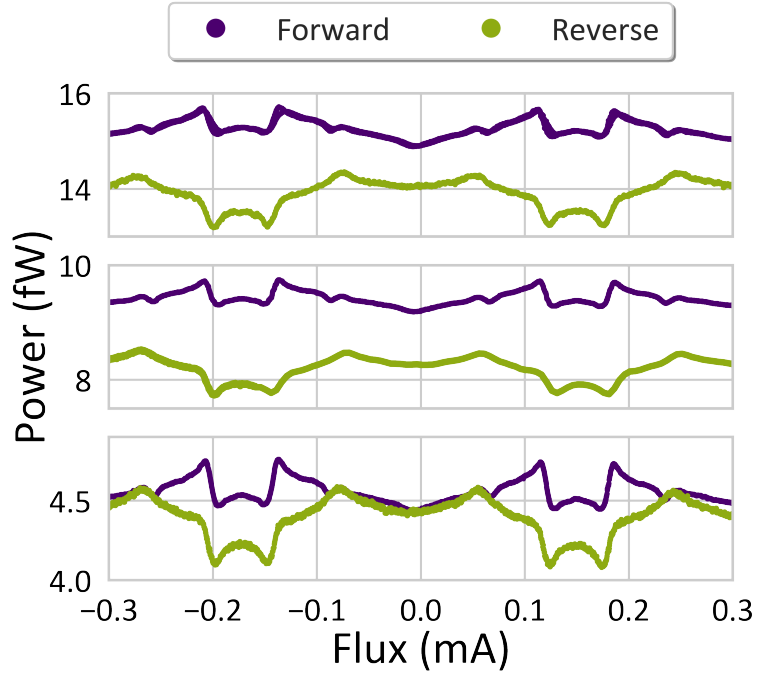


Figure 2. Tuneable transport

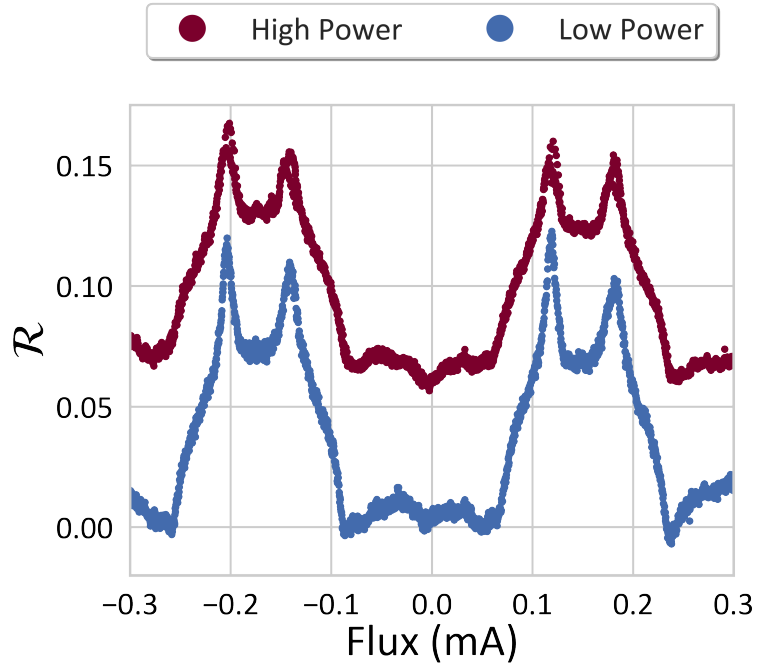


Figure 3. Rectification Ratio